MCAO Magnification Control for Optimal Point Source Sensitivity

Glen Herriot*[a], Ryuki Suzuki[b], Jean-Pierre Véran[a], Lianqi Wang[c], Gelys Trancho[c]
[a]Herzberg Astronomy Astrophysics, 5071 W. Saanich Rd, Victoria BC, Canada V9E 2E7
[b]National Astronomical Observatory Japan, 2 Chome-21-1 Osawa, Mitaka, Tokyo 181-0015, Japan
[c]Thirty Meter Telescope, 100 W. Walnut St., Suite 300, Pasadena CA, USA 91124

ABSTRACT

We present the tradeoff between telescope plate scale control with MCAO and point source sensitivity. Conventional thinking about MCAO assumes that an asterism of natural guide stars is the reference for magnification of the science image. If the guide stars appear displaced radially on their WFSs, then applying opposing focus modes on two DMs will resize the image and restore the guide stars to their desired position on the WFSs. However, telescope and instrument magnification errors, star catalog errors, and positioning errors of probes (calibrated with a focal plane pinhole mask) should also be compensated. But deformable mirrors have limited stroke available for such correction. Furthermore, changing the image size means varying the output f/ratio and thus the pupil image size on an instrument's Lyot stop. The result is additional background (for an undersized pupil image) or alternately and even worse an undersized mask relative to an enlarged telescope pupil image, with a severe impact on sensitivity proportional to the square of the diminished Strehl ratio. Optimizing the tradeoff among these effects leads us to propose that the de facto reference for image scale should be the size of the pupil image on the Lyot mask including its as-built pupil imaging optics. We describe calibration and control methods to achieve this, incorporating pinhole mask, DM pokes, pupil viewing camera and pyramid WFSs.

Keywords: Point Source Sensitivity, MCAO, Lyot Mask, Pyramid WFS

1. INTRODUCTION

An asterism of natural guide stars is conventionally the plate scale (magnification) reference for an MCAO science image. But relying on guide stars as the prime reference for plate scale (image magnification) control may cause an unacceptable observing time penalty as explained below.

1.1 Background

NFIRAOS[1] for TMT is an MCAO system that feeds its first-light client instrument IRIS[4], an imaging spectrograph. MCAO uses natural guide stars (NGS) to control image tip, tilt and focus, and also to control plate scale and image rotation. IRIS has three On-Instrument Wavefront Sensor (OIWFS) guide probes, which may be individually configured as imagers (tip/tilt sensors) or as 2x2 Shack-Hartmann sensors. At the beginning of an observation, these probes are prepositioned to measure tip-tilt on three stars, with at least one of them set up to measure focus as well. These stars are selected when planning observations, and rely on catalog positions. In operation, the OIWFS pixels are streamed to the NFIRAOS Real-Time Controller. To change or correct the image magnification seen at IRIS, NFIRAOS puts an opposing focus mode on its two DMs, conjugate to ground and 11.2 km respectively, so that the three NGS stars are steered to the null points of the OIWFSs. Errors in positioning the probes (calibrated with a focal plane pinhole mask) and guide star position errors in the catalog will change the image plate scale improperly in IRIS.

Moreover, TMT allocates only 2 μm RMS OPD DM stroke for all quasi-static optics errors including plate scale correction. Plate scale correction has to compensate for catalog and probe errors as well as telescope as-built focal length errors and their drift. Telescope optics will be calibrated and reset biweekly using the Alignment and Phasing System (APS) that sights along the telescope elevation axis and delivers an optimized image to APS. Differences in axial position of NFIRAOS w.r.t. APS, as well as thermal expansion of the steel telescope will put NFIRAOS at a different radius from the TMT tertiary mirror -- refocusing with M2 will change the telescope f/ratio. Similarly mechanical and optical tolerances of IRIS w.r.t. the output focus of NFIRAOS will, after refocusing the science image with the DMs, change the delivered f/ratio.

Furthermore, changing the image size in IRIS means varying the NFIRAOS output f/ratio and thus changes the pupil size on an instrument's Lyot stop. The result is additional background (for an undersized pupil image) or alternately and even worse an undersized mask relative to an enlarged telescope pupil image, with a severe impact on sensitivity proportional to the square of the diminished Strehl ratio.

The RMS total of the current end-to-end tolerances from M1 to the IRIS imager detector results in approximately 0.4% RMS variation of diameter of the pupil image on IRIS's pupil mask. The biggest contributor is the as-built telescope effective focal length tolerance that accounts for 0.36%, mostly due to figuring errors on optics radius of curvature. Correcting this purely with DMs would require ~6 μm RMS mechanical stroke, but the DMs are only capable of 10 μm peak-valley.

NFIRAOS had long planned to offload plate scale errors from the DMs to the telescope, which would change the radius of curvature of the primary mirror and refocus the secondary mirror. But, this in turn will mean that the primary mirror segments no longer perfectly fit the new radius of curvature, introducing uncorrectable high-frequency wavefront errors: 'scalloping'. For 75 ppm of plate scale, the DM requires 1 micron rms OPD of stroke, while correcting it with the telescope will create 62.5 nm RMS WFE of scalloping mode. As a result, current plans are to avoid plate scale offload from NFIRAOS to the telescope with techniques described below.

2. IMAGE MAGNIFICATION, F/RATIO, AND PUPIL SIZE

2.1 Relationships

NFIRAOS' optics image the TMT pupil (the primary mirror M1) onto DM0. Within IRIS there is a pupil relay that reimages the ground-conjugated DM0 onto IRIS' Lyot mask. IRIS also has a deployable pupil viewing camera. These are illustrated in Figure 1 that also shows one of the OIWFS in the upper left.

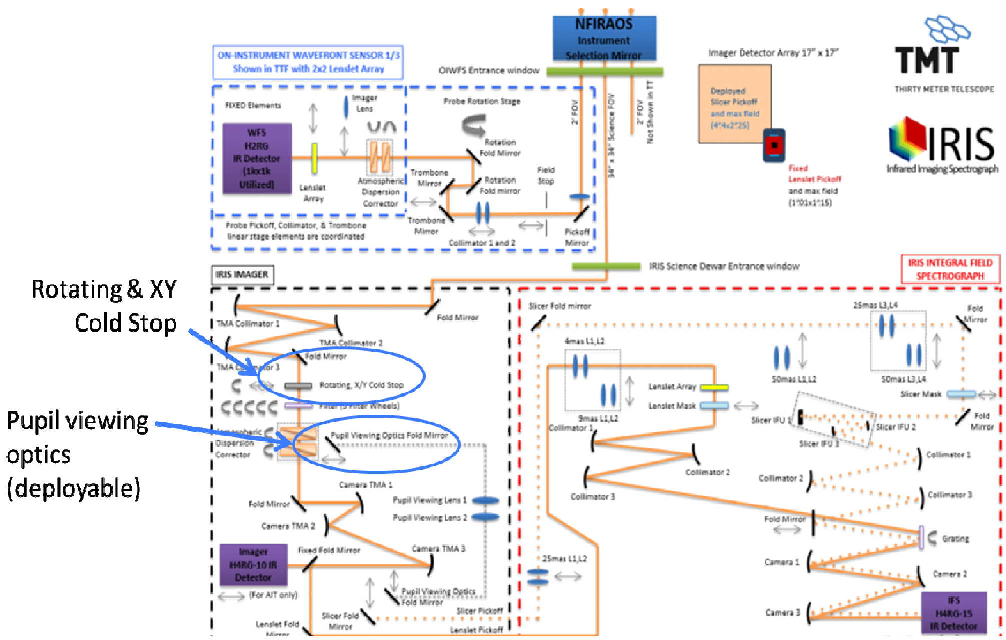

Figure 1 Block diagram of IRIS.

The TMT-design f/ratio is f/15, and NFIRAOS is designed to also deliver an f/15 beam to its three client instrument ports. Magnification of the science image is linearly proportional to the f/ratio, as is the apparent diameter of the exit pupil from NFIRAOS. It is important to realize that when NFIRAOS changes its output f/ratio (or image magnification) with its two DMs, that the pupil image relayed onto IRIS' Lyot mask also changes diameter linearly.

2.2 Point source sensitivity

Point source sensitivity is defined as the inverse of observing time, normalized to that of a perfect telescope. In near-IR instruments, Lyot masks are typically slightly undersized compared to the pupil image size to ensure that they block background light despite alignment and manufacturing tolerances. Undersizing causes vignetting that costs throughput, which decreases observing efficiency proportional to area loss. But a larger effect is that undersizing increases the full width at half-maximum of the point spread function, decreasing sensitivity proportional to the square of Strehl ratio relative to that for the full telescope aperture (see Figure 2). As a rule of thumb for TMT, if a Lyot mask is undersized by 1% on radius, it costs 30% of observing time for background limited point sources[1].

Similarly if NFIRAOS enlarges the delivered image in an otherwise perfect system, then the pupil relay in IRIS will oversize the pupil image with respect to the mask diameter, and cost observing time. This is an asymmetric penalty: if the f/ratio is too small (pupil image is too small): then excess background will be admitted, and the science image may be undersampled, but there are no throughput nor Strehl Ratio losses.

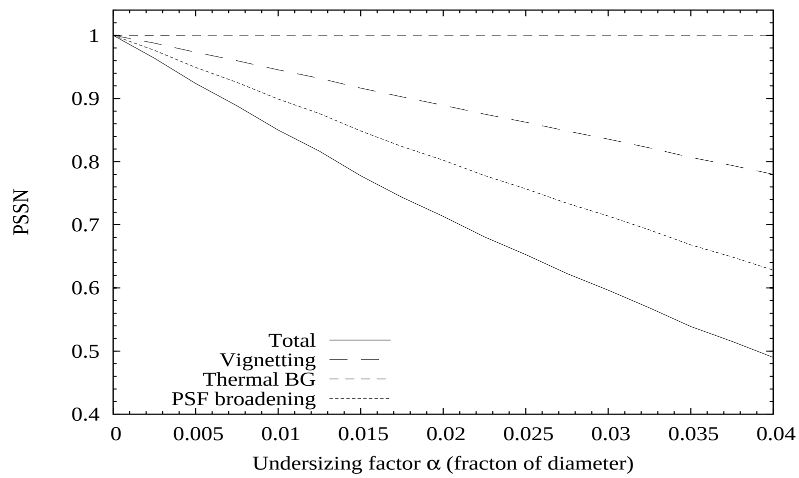

Figure 2 Loss of point source sensitivity (PSSN) due to Lyot mask undersizing

3. CONTROL SCHEME

3.1 Operating principle

The key concept is to treat the as-built Lyot mask as the quasi-static reference for plate scale. Even if the mask is the wrong size, or if any of the upstream optics and mechanics conspire to produce an incorrect plate scale, the control system will force the pupil image on the Lyot mask to be the right size to match the mask. This will optimize PSSN. If the mask is dimensionally stable, and the optics downstream of the mask are stable, then every science exposure will have the same magnification. Although of course, this magnification may be wrong, but the astrometry procedures and error budget for the most demanding cases with TMT NFIRAOS and IRIS assumes at least three references (e.g quasars or GAIA stars) are in each exposure on the 34 arcsecond square imaging detector[5]. The plan is to rescale the images to match these references during post-processing.

3.2 Signal Flow

In Figure 3 we see a schematic of NFIRAOS and the input sections of IRIS. The telescope light arrives from the top of the diagram and reflects off the high-altitude and ground-conjugated deformable mirrors. Then image forming optics create the output focal plane that IRIS receives. At the focal plane, IRIS' three On-Instrument WFS probes measure T/T on three natural guide stars. These measurements enter the Real Time Computer (RTC) which controls the DMs. If the diameter of the best fit circle through the measured positions of the NGS stars does not match the size expected from the best fit circle through the guide star catalog positions, then the RTC will change magnification by applying opposing focus shapes on the DMs at high bandwidth. The amount of focus over the footprint of a point source is an identical amplitude on each DM, to preserve a constant focus at the focal plane. But of course, the total peak to valley on DM11 is higher because of the larger metapupil. Additional power on DM0 will null the focus seen on one of the guide probes that is configured in T/T/F mode. Although it is not a subject of this paper, differential magnification of X versus Y and also -45 versus 45 degrees is also compensated by opposing astigmatism modes on the two DMs. Differential magnification mostly comes from atmospheric turbulence, star catalog errors and probe position errors, and not quasi-static optics errors, assuming that TMT is built to its specifications.

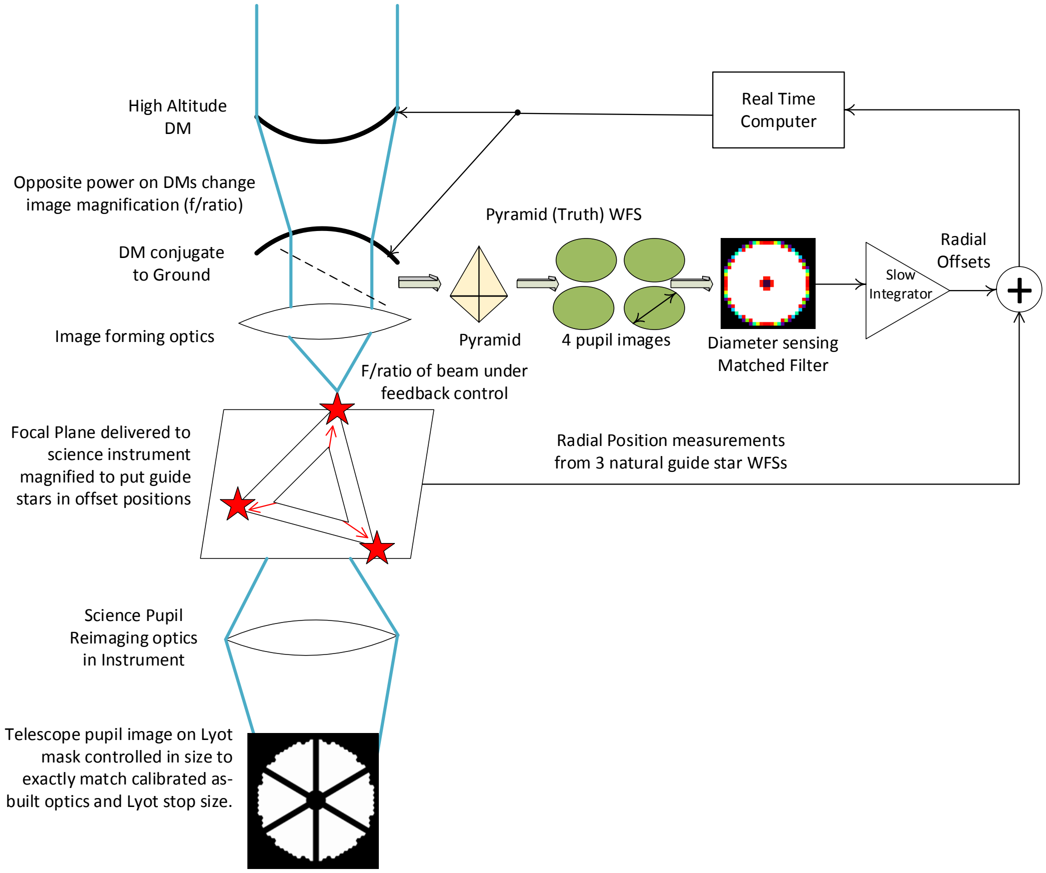

Figure 3 Block Diagram of Plate scale control for NFIRAOS/IRIS

3.3 Background magnification control task

Meanwhile, NFIRAOS has a Pyramid WFS[7] that receives light in the 600 to 800 nm bandpass (Figure 6). This PWFS serves as a truth WFS in laser guide star operation to sense wavefront error modes that are not properly measured by the six laser WFSs due to uncertainties in the structure of the sodium layer, Rayleigh scattering and calibration errors. This wavefront sensing signal path is not depicted in Figure 3. However, as usual for a PWFS, its optics create four pupil images on a detector. As well as being used for sensing wavefront, these images are also processed to measure their size using diameter-sensing matched filters, which are created offline in advance as described in section 4.

Taking the dot-product of all the pixel intensities times the matched filter generates a magnification error signal. This is integrated with low gain to form a correction signal that is then projected onto radial tip/tilt offsets and added to the OIWFS T/T measurements. The main integrator in the RTC control loop then drives these inputs to zero, to magnify the pupil images in the PWFS to the size established by the daytime calibration procedure. Note that two integrators alone in series always create an unstable closed loop system; following established design practice, there is a lead filter compensator (not shown) after the slow integrator before the projection onto radial offsets.

4. DAYTIME CALIBRATION

4.1 DM11 pokes

What we really want to do is to control the pupil size on the Lyot mask, not necessarily on the PWFS detectors. Starting from the pupil mask we will establish a daytime metrology chain to reference the PWFS pupil's size to IRIS' mask.

The process begins by deploying a point source at the telescope focal plane located just inside the front window of NFIRAOS. We flatten DM0 and poke a waffle pattern on DM11. Figure 4 shows the resulting uniform wavefront amplitude and waffly phase at DM11.

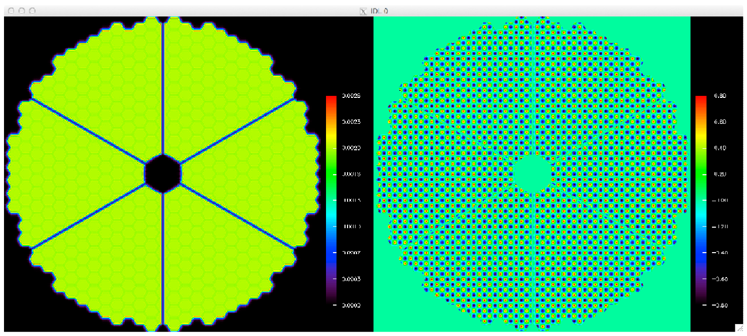

Figure 4 Wavefront at DM11 after adding 1.5um P-V waffle on DM11. Left: amplitude. Right: phase.

Then by Talbot propagation to the pupil plane, conjugate to DM0 and also to the Lyot mask, some of this phase at D11 is converted to amplitude. High spatial frequencies of waffle pattern have propagated to amplitude. Phase still largely contains waffle, with slightly increased amplitude as shown in Figure 5.

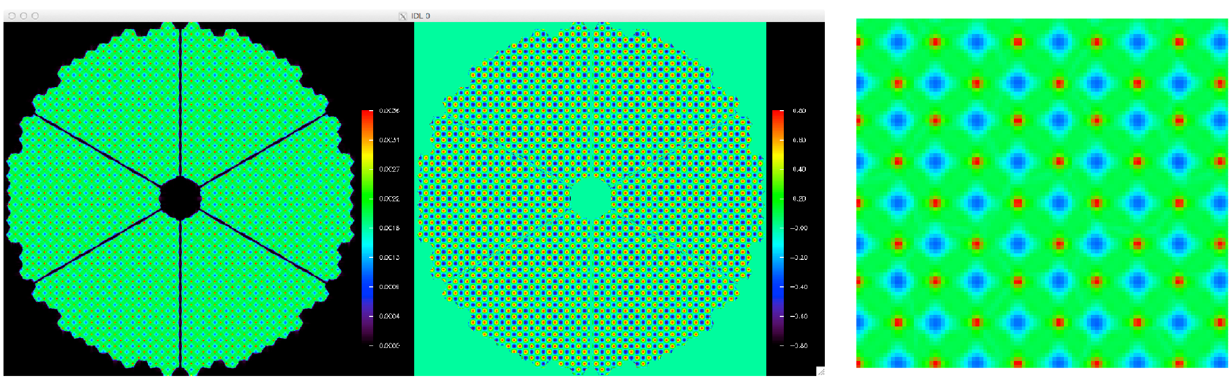

Figure 5 Wavefront after Talbot propagation from DM11 to pupil plane. Left: amplitude. Centre: phase. Right: Detail of amplitude

4.2 Pupil viewing camera

Deploying the pupil viewing camera within IRIS we expect to see an image like the left hand panel Figure 5. The silhouette of the Lyot mask includes the serrated TMT primary mirror, the secondary mirror and its spiders. Since NFIRAOS has exactly 60 actuator pitches across the pupil, we expect to see exactly 60 spot pitches across the mask. We will iterate the output f/ratio from NFIRAOS by adjusting opposing focus shapes (superimposed on DM11 waffle) to both DMs until we do see 60. This will account for optical tolerances and mask manufacturing tolerances in IRIS and NFIRAOS.

4.3 Magnification sensing matched filter

When we do have the correct magnification at the pupil viewing camera, then we will save an image from the PWFS detector. We will also deliberately change the pupil magnification by a known amount (e.g. 0.1%) and save another image. The difference in these two images is a measure of the derivative of PWFS pixel intensities versus magnification changes. With these two ingredients we can create a magnification-sensing matched filter to apply to the PWFS pupil images in real time on-sky.

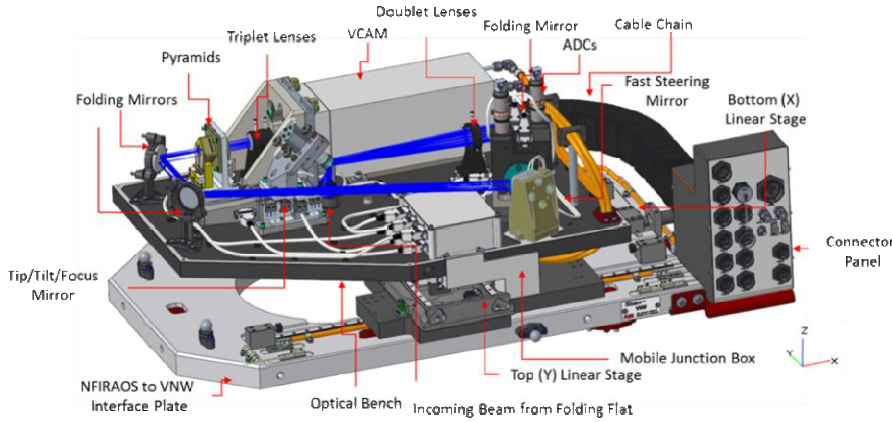

Figure 6   NFIRAOS PWFS on its XY stage. VCAM is the CCD camera.

5. DISCUSSION

NFIRAOS cam stabilize moderate plate scale variation with DM stroke budget allocation for quasi-static errors. However, as noted in section 1.1, the largest source of magnification uncertainty seen at the Lyot mask is the as-built telescope effective focal length which exceeds the stroke budget. We won't know the end-to-end pupil image size on IRIS' Lyot mask until we commission on sky. One suggestion to maximize sensitivity is to make pupil size measurements on sky and then warm and open IRIS and install a newly cut Lyot mask to suit the telescope. This will occur on the critical path during commissioning and so it not attractive. We are also working with TMT to explore tightening the telescope optics radius of curvature tolerances, but this is less likely to succeed at solving the entire problem. It has not escaped our attention that this method could be extended to differential magnification in XY and 45 degrees.

6. CONCLUSIONS

We have described a method that optimizes observing efficiency by relying on an instrument's as-built Lyot mask as the static reference for image scale, rather than NGS guide star catalogs which may suffer from astrometric errors. Then we depend on post-processing of science images to account for low-order image distortion like magnification errors resulting from e.g. mask fabrication errors propagating according to the methods presented here. Thus we can minimize the observing time penalty incurred by having a mismatch between a Lyot stop diameter and the pupil image on it.

REFERENCES

[1] Herriot, G., "Point Source sensitivity, Pupil alignment, Calibration and Control for TMT-NFIRAOS-IRIS," AO4ELT5 (2017)

[2] Véran, J.-P. and Herriot, G., "Telescope Pupil Tracking using a Pyramid WFS", AO4ELT5 (2017)

[3] Crane, J. "NFIRAOS adaptive optics for the Thirty Meter Telescope", Proc. SPIE 10703, (2018).

[4] Larkin, J. et al., "The Infrared Imaging Spectrograph (IRIS) for TMT: instrument overview," Proc. SPIE 9908, (2016)

[5] Schoeck, M., "Flowdown of the TMT astrometry error budget(s) to the IRIS design," Proc. SPIE 9908, (2016)

[6] Véran, J.-P. "NFIRAOS Calibration Plan Update", AO4ELT6 (2019)

[7] Cournoyer, Al, "Final design of the NFIRAOS Visible Natural guide star Wavefront sensor (VNW) for the Thirty Meter Telescope",